

Research Article

The Role of Foaming Agent and Processing Route in Mechanical Performance of Fabricated Aluminum Foams

Alexandra Byakova,¹ Iegor Kartuzov,¹ Svyatoslav Gnyloskurenko,² and Takashi Nakamura³

¹ Institute for Problems of Materials Science, National Academy of Sciences of Ukraine, Kiev 03142, Ukraine

² Physical-Technological Institute of Metals and Alloys, National Academy of Sciences of Ukraine, Kiev 03142, Ukraine

³ Institute of Multidisciplinary Research for Advanced Materials, Tohoku University, Sendai 980-8577, Japan

Correspondence should be addressed to Svyatoslav Gnyloskurenko; slava.vgn@gmail.com

Received 18 December 2013; Revised 4 March 2014; Accepted 5 March 2014; Published 31 March 2014

Academic Editor: Alexander Tsouknidas

Copyright © 2014 Alexandra Byakova et al. This is an open access article distributed under the Creative Commons Attribution License, which permits unrestricted use, distribution, and reproduction in any medium, provided the original work is properly cited.

The results of this study highlight the role of foaming agent and processing route in influencing the contamination of cell wall material by side products, which, in turn, affects the macroscopic mechanical response of closed-cell Al-foams. Several kinds of Al-foams have been produced with pure Al/Al-alloys by the Alporas like melt process, all performed with and without Ca additive and processed either with conventional TiH_2 foaming agent or CaCO_3 as an alternative one. Damage behavior of contaminations was believed to affect the micromechanism of foam deformation, favoring either plastic buckling or brittle failure of cell walls. No discrepancy between experimental values of compressive strengths for Al-foams comprising ductile cell wall constituents and those prescribed by theoretical models for closed-cell structure was found while the presence of low ductile and/or brittle eutectic domains and contaminations including particles/layers of Al_3Ti , residues of partially reacted TiH_2 , and Ca bearing compounds, results in reducing the compressive strength to values close to or even below those of open-cell foams of the same relative density.

1. Introduction

Remarkable absorbing ability resulted from capacity of closed-cell aluminum foams to undergo large strains (up to 60–70%) under almost constant stress offers significant performance gains for crash protection and other applications where effective utilizations of impact energy are required [1]. For instance, in aluminum foam sandwich (AFS) structures composed of metal/ceramic coversheets and Al-foam core, the last one is an efficient impact energy absorber that limits accelerations in crash accidents, providing crash protection for terrestrial and marine vehicles [2, 3]. That is why there has been an extensive interest in the production [1, 4–10] and mechanical performance of Al-foams [11–16].

Despite continuous efforts, the production processes for Al-foams suffer technical and economical limitations. As applied to the high-usage production methods based on handling of a melt and powder compact technique [4, 10] economical limitation arises particularly due to the employing of costly conventional foaming agent, titanium hydride (TiH_2).

In addition, expensive granulated Ca used as thickening agent contributes in material cost of Al-foam produced by conventional melt processing like Alporas route [17] while rather expensive gas atomized Al/Al alloy powder leads to increasing the material cost of the precursor and therefore products manufactured via powder compact technique [4, 10]. Because of this there is a strong motivation to develop cost effective processing routes. At this point cheap calcium carbonate (CaCO_3) as alternative foaming agent has been originally proposed by the researches in Japan in the developing the Alporas route [6] and later its applicability has been extended for powder compact technique [5, 6, 9]. In addition, melt processing like Alporas route that provides the increasing melt effective viscosity with no admixture of granulated Ca has been recently developed [18]. Nevertheless, transfer of Al-foam in engineering practice cannot be done without a detailed knowledge of the Al-foam properties (including mechanical ones) and limits of foaming processes.

It is of common knowledge that the most important microstructural feature affecting the mechanical properties

is relative density, the ration of density of the foam to that of the solid, ρ/ρ_s . Several approaches based on an idealized representation of a defect-free cellular structure have been developed for interpreting mechanical behavior of foams. Among those are the high-usage approaches for describing mechanical properties of ideal open- and closed-cell foams which are summarized in [11]. The simplest approach is based on dimensional arguments and gives the dependence of properties on relative density and on cell wall properties but not on cell geometry [19]. The complex cell geometry of foams is difficult to model accurately. At this approach the constants relating to cell geometry are usually found by fitting the model equations to experimental data. The second method that approximates the unit cell as tetrakaidecahedron is capable of estimating geometrical constants by using either structural mechanics or finite element analysis [20–23]. The third approach based on spatially periodic arrangement of several random Voronoi cells by using finite element analysis [24] provides the best representation of foams cell geometry. Cell unit with flat faces are usually used in the models.

However, the actual profile of mechanical properties for real Al-foams is far removed from theoretical predictions based on idealized representations of defect-free cellular materials [11]. In particular, a number of available cellular materials and especially closed-cell foams yield at a relatively strength that is lower than that predicted by theoretical models [11, 19]. The scattering of the mechanical properties impedes practical applications of foams [25, 26].

It is commonly considered that disagreements between experimental results and theoretical predictions arise due to different structural imperfections existing in real metallic foams. Combination of synchrotron X-ray microtomography and mechanical analysis including finite element simulation elucidates the influence of structural imperfection on mechanical performance of foams [11, 27–32]. In particular, deformation mechanism of foams depends strongly on the cell morphology whilst the effect of the cell size is negligible [27, 29, 32]. Irregularities in the cell shape on mesoscopic level can induce localized bending. For instance, X-ray microtomography indicates that highly elliptical cells with T-shape can induce bending in the neighboring cell walls, initiating the collapse of deformation bands [11, 27]. Finally, curvature and corrugation of cell faces [26, 28] and micropores and their spatial distribution in cell walls [33] as well as nonhomogeneous density distribution [29, 34] and fractured cell walls [11, 35] are considered to be the key factors in control of mechanical behavior of aluminum foams. However, it is difficult to quantify the precise significance of these factors because of microscopic features such as foreign particles, precipitates, and solute elements present in the cell wall material, currently thought to be also of great importance, resulting at least in the nonhomogeneous stress/strain distribution. Nevertheless, the microstructural aspects (especially those referred to mechanical properties of the cell wall constituents) are still largely ignored in most studies, despite the known fact that microstructural features would have dramatic effects on the performance characteristics of corresponding bulk material.

This problem becomes increasingly pronounced when foaming processes are performed with gas-releasing agent and other additives, resulting in unconventional matrix alloy comprising great number of various intermetallic compounds and other foreign particles [2, 8, 11, 36]. Great number of various intermetallic compounds and other foreign particles formed in the course of the foaming process substantially affect the micromechanism of deformation, degrading the mechanical response of foams [2, 14, 15, 36]. Unfortunately, evidence concerning the mechanical response of Al-based intermetallic compounds and other particles, typical for the cell wall material of aluminum foams, is few in number [16, 36].

This effort is to elucidate the role of processing additives in influencing the mechanical performance of Al-foams processed with different kinds of parent Al-alloys via Alporas route. Attention is primarily concentrated on the effect of damage behavior of cell wall constituents induced by processing additives on macroscopic compressive behavior of Al-foam.

2. Materials and Experimental Procedure

2.1. Materials. Several kinds of closed-cell foams marked as F1–F14 and listed in Table 1 were used in experiments. Pure aluminum (purity 99.95) and several conventional Al-alloys were used as matrix materials. Foams 1 and 2 were processed with pure aluminum, whereas the foams F3–F6 were processed with cast Al-7Si alloy (similar to A356 alloy). Wrought alloy with elementary composition of Al-1Mg-0.6Si-0.28Cu-0.2Cr (similar to 6061 alloy) and Al-5Mg alloy (similar to 5356 alloy) were employed to produce the foams F7, F8, F9, and F10, respectively. In addition, Al-Zn-Mg alloy with composition of Al-5.5Zn-3Mg-0.6Cu-0.5Mn doped additionally by small amount (<0.6 wt.%) of Sc and Zr (similar to 7075 alloy) was also chosen as a parent material for fabrication of F11–F14 foams.

All kinds of Al-foams were produced via Alporas like route in which either titanium hydride TiH_2 or calcium carbonate $CaCO_3$ were employed as foaming agents [9, 14, 15]. In addition, both hydride and carbonate Al-foams were produced either with or without Ca additive introduced usually into melt as thickening agent. All kinds of Al-based foams were performed by cylindrical blocks of 90 mm in diameter and 180 mm in height. A number of samples were directly machined from each kind of as-received foamed materials to use them for structural characterization and testing. Sample dimensions were about $20 \times 20 \times 30 \text{ mm}^3$ and $30 \times 30 \times 45 \text{ mm}^3$.

In addition, several solid alloys of compositions roughly corresponded to those formed in the cell wall materials of the studied Al-foams were fabricated by casting to use them in the experimentation. Approximated values of yield strength for these solid materials, listed in Table 1, were determined by the conventional mechanical tests in tensile to use them as input data in theoretical models for interpreting the behavior of foam under compression.

TABLE I: Characteristics for different kinds of Al-based foams produced by Alporas like route.

Foam code	Processing variables (alloy and additives) wt.%	Relative density (ρ/ρ_s) ¹	Cell size, mm	Solid yield strength, σ_{ys} (MPa)
F1	Al + 1TiH ₂ + 1Ca	0.21–0.37	3.1 ± 0.9	42.8 ± 4.89
F2	Al + 2CaCO ₃ + 1Ca	0.24–0.09	1.5 ± 0.6	43.5 ± 7.12
F3	Al-7Si alloy + 1.5TiH ₂ + Ca	0.17–0.30	3.0 ± 0.4	220 ± 20.54
F4	Al-7Si alloy + 1.5TiH ₂	0.17–0.24	3.2 ± 0.5	180 ± 21.68
F5	Al-7Si alloy + 2CaCO ₃ + 1Ca	0.18–0.29	1.5 ± 0.5	195 ± 19.53
F6	Al-7Si alloy + 2CaCO ₃	0.18–0.27	1.7 ± 0.6	140 ± 15.67
F7	Al-1Mg-0.6Si alloy + 1.5TiH ₂ + 1Ca	0.15–0.26	2.1 ± 0.6	120 ± 14.82
F8	Al-1Mg-0.6Si alloy + 1.5TiH ₂	0.25–0.43	2.3 ± 0.7	100 ± 9.85
F9	Al-5Mg alloy + 1.5TiH ₂ + 1Ca	0.18–0.32	3.6 ± 0.5	180 ± 19.73
F10	Al-5Mg alloy + 1.5TiH ₂	0.31–0.40	3.5 ± 0.6	160 ± 17.13
F11	Al-Zn-Mg alloy + 1.5TiH ₂ + 1Ca	0.22–0.38	2.1 ± 0.7	560 ± 28.24
F12	Al-Zn-Mg alloy + 1.5TiH ₂	0.19–0.40	2.3 ± 0.6	540 ± 26.15
F13	Al-Zn-Mg alloy + 2CaCO ₃ + 1Ca	0.20–0.34	1.1 ± 0.5	575 ± 29.48
F14	Al-Zn-Mg alloy + 2CaCO ₃	0.20–0.33	1.2 ± 0.6	531 ± 15.14

¹ ρ and ρ_s correspond the density of foam and bulk solid, respectively.

2.2. Structural Characterization. All samples machined from the studied kinds of Al-foams were characterized by their relative density ρ/ρ_s (where ρ and ρ_s correspond to the density of foam and solid, resp.), cell morphology, and cell wall microstructure. Relative density, ρ/ρ_s , was measured by weighing a sample of known volume. Range of relative density for the samples machined from the studied kinds of Al-foams is listed in Table I. Cell morphology, including cell size and shape, was studied by using scanned images of cellular structure for each kind of the studied Al-foams. Cell size indicative of the studied kinds of Al-foams is presented in Table I. Microstructure of cell wall materials for the studied Al-foams was investigated using scanning electron microscopy (SEM) in both secondary and back-scattered modes. Material elementary composition was studied using energy dispersive X-Ray spectroscopy (EDS) and electron probe microanalysis (EPMA).

2.3. Mechanical Testing. Deformation behavior of Al-foams was examined under uniaxial compressive tests performed on prismatic specimens with dimensions either $20 \times 20 \times 30 \text{ mm}^3$ or $30 \times 30 \times 45 \text{ mm}^3$. The minimum dimension of particular specimen in each of three directions was seven times more than the cell size to avoid size effect. The compression tests were performed on a servohydraulic testing machine under displacement control and static strain rate of $1.5 \times 10^{-3} \text{ s}^{-1}$.

3. Results and Discussion

3.1. Material Characterization. All kinds of the studied Al-foams were believed to have closed cells of roughly spherical shape [14]. However, homogeneity of the cellular structure and mean cell size for carbonate foams (F2, F5, F6, F13, and F14) are found to be at least two times smaller than that for

hydride ones (F1, F3, F4, F11, and F12) processed with the same parent alloys, as evidenced from Table I.

Figure 1 shows microstructure of cell wall materials for several kinds of Al-foam. Cell walls of foams (F1–F10) based on pure Al and Al alloys with compositions Al-7Si, Al-1Mg-0.6Si, and Al-5Mg consist of coarse Al dendrites rounded by a network of eutectic domains (light grey), as was originally shown in [8, 14, 16, 36]. Interdendritic network of redundant phase being emerged in a matrix of Al solid solution with randomly scattered Al₃(ScZr) intermetallic particles is characteristic for the foams (F11–F14) processed with Al-Zn-Mg-alloys [14, 15, 36].

Excluding carbonate kinds of Al-foams (F2, F6, F13, and F14) cell wall materials for all other foams exhibit a lot of foreign particles. In Al-foams (F3 and F5) based on Al-7Si alloy and processed with Ca additive, coarse crystals compositionally corresponded to Al₂CaSi₂ intermetallic compound (1) and are presented in the cell wall material besides E (Al + Si) eutectic domains (2), as can be seen in Figure 1(a). Formation of needle-shaped Al₂CaSi₂ crystals (5) is also detected in the cell wall material of Al-foam based Al-1Mg-0.6Si alloy (F7), as shown in Figure 1(b). Foreign particles of partly converted TiH₂ and/or its reaction products such as particles/layers Al₂Ti/Al₃Ti (12) are randomly distributed in the cell walls of hydride kinds of Al-foams (F1, F3, F4, and F7–F12). In line with [14] the above Ti-rich particles are mainly presented in the cell wall material of hydride kinds of Al foams (F4, F8, F10, and F12) processed without Ca additive, as can be seen in Figure 1(d).

The results of elementary distribution show that composition of eutectic domains formed in the cell wall material of other Al-foams was found to be rather different compared to those of parent alloys and dependent on the processing additives. Generally, dissolved Ca is largely accumulated within the eutectic domains/redundant phase, resulting in their local modification with formation of foreign Ca-bearing

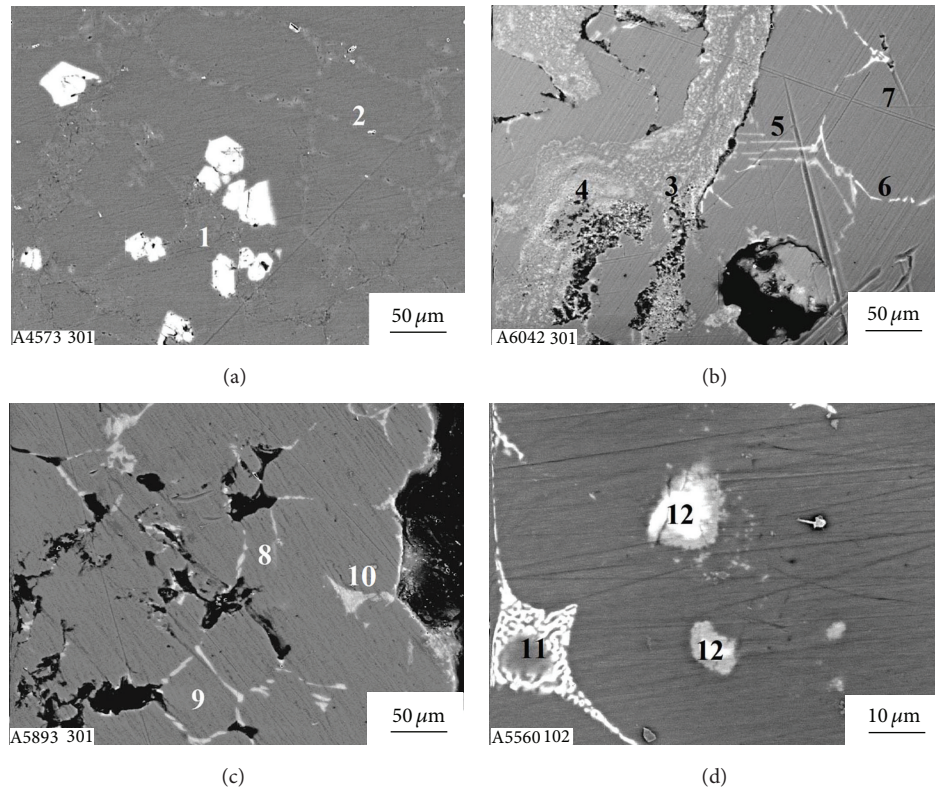


FIGURE 1: SEM micrographs of cell wall materials for Al-foams processed either with (a) CaCO_3 or with (b)–(d) TiH_2 and performed (a)–(c) with and (d) without Ca additive and performed with different parent alloys: (a) Al-7Si (F5), (b) Al-1Mg-0.6Si (F7), (c) Al-5Mg (F9), and (d) Al-Zn-Mg (F12).

eutectic zones. In particular, besides $\text{E}(\alpha\text{-Al} + \text{Mg}_2\text{Si})$ eutectic domains (6) indicative of parent Al-1Mg-0.6Si alloy, foreign eutectic zones such as $\text{E}(\alpha\text{-Al} + \text{Al}_4\text{Ca})$ (3), $\text{E}(\alpha\text{-Al} + \text{Al}_4\text{CaCu})$ (4), and $\text{E}(\alpha\text{-Al} + \text{Al}_2\text{CuMg})$ (7) are formed in Al-foam (F7), as shown in Figure 1(b). The same is true for Al-foam (F9) processed with Al-5Mg alloy. Cell wall material of Al-foam (F9) comprises Ca-bearing eutectic zones such as $\text{E}(\alpha\text{-Al} + \text{Mg}_2\text{Ca})$ (9) and $\text{E}(\alpha\text{-Al} + \text{Al}_4\text{Ca} + \text{Al}_3\text{Ti})$ (10) besides $\text{E}(\alpha\text{-Al} + \text{Mg}_5\text{Al}_8)$ eutectic domain (8) indicative of parent alloy, as shown in Figure 1(c). In addition, small amount (roughly about 0.26 at.%) of Ti solutes in Al matrix of hydride kinds of Al-foams. The latter is also concentrated within the eutectic domains, resulting in formation of Al_3Ti compound. As an example, Ti-bearing eutectic zones such as $\text{E}(\alpha\text{-Al} + \text{Al}_4\text{Ca} + \text{Al}_3\text{Ti})$ (10) and $\text{E}\{\alpha\text{-Al} + \text{T}(\text{AlCuMgZnTi})\}$ (11) are found in the cell walls of Al-foams (F9 and F12) based on Al-5Mg and Al-Zn-Mg alloys, respectively, as shown in Figures 1(c) and 1(d).

The important point concerns the difference in damage behavior of cell wall constituents comprised by cell wall materials of different kinds of Al-foams. In particular, Al + Al_4Ca eutectic domains indicative of carbonate kind of Al-foam (F2) processed with pure Al demonstrate quite high plasticity that is close to $\alpha\text{-Al}$ dendrites, whereas those indicative of all another kinds of Al-foams show low ductility and/or high brittleness [14, 16, 36]. Crumbling out the brittle eutectic domains/redundant phase occurs even after slightly slicing

the specimen, as can be seen in Figures 1(a) and 1(c). The same is true for contaminations including particles/layers of Al_3Ti , as well as residues of partially decomposed TiH_2 and Ca-bearing compounds. The data published in [16, 36] indicate that the solid materials, which compositionally corresponded to the above cell wall contaminations, demonstrate rather low ductility. Moreover, the latter solids show extremely small fracture toughness, K_{Ic} , although their strength is quite high. In particular, fracture toughness ($K_{Ic} = 1.71 \pm 0.18$) of titanium hydride TiH_2 is even less than that for technical glass ($K_{Ic} = 1.17 \pm 0.09$) [16]. This suggests that the presence of low ductile and/or brittle cell constituents can lead to impairing damage resistance of the cell walls, facilitating their premature failure under loading.

3.2. Compressive Response of Al-Foams. All kinds of Al-foams display a macroscopic mechanical response rather similar to elastic/plastic behaviour [1, 2, 11, 19]. However, different kinds of Al-foams exhibit considerable differences in microscopic deformation events at the “plateau” regime, as can be seen in Figures 2(a) and 2(b).

Figure 2(b) shows that carbonate kind of foam (F2) with ductile Al + Al_4Ca eutectic domains in the cell wall material [14, 16, 36] deforms smoothly which is typical for plastic buckling [11, 19]. In contrast to this slight hardening/softening effects superimposed upon an increasing “plateau” stress level

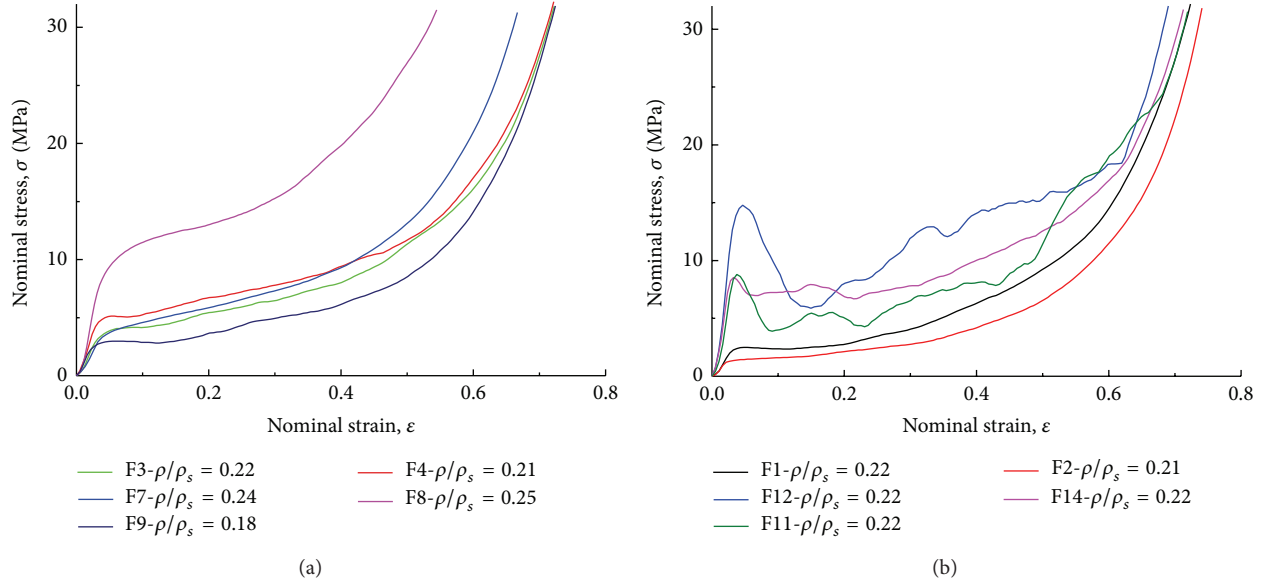


FIGURE 2: Compressive stress-strain curves for hydride (F1, F3, F4, F11, and F12) and carbonate (F2 and F14) kinds of Al/Al-alloy foams processed with (F1-F3, F7, and F11) and without (F4, F8, F12, and F14) Ca additive: (a) Al-foams based on Al-7Si alloy (F3 and F4), Al-1Mg-0.6Si alloy (F7 and F8), Al-5Mg alloy (F9); (b) Al-foams based on pure Al (F1, F2) and Al-Zn-Mg alloy (F11, F12, and F14).

is seen in deformation patterns of hydride kinds of Al-foams (F1, F3, F4 and F9) processed with pure Al and Al alloys such as Al-7Si and Al-5Mg. These deformation events are usually ascribed to the cell walls local failure being stimulated by crushing the low ductile eutectic domains and brittle foreign particles [12, 14, 34]. Hydride kinds of Al-foams (F11, F12) processed with Al-Zn-Mg alloy, whose cell walls comprise a high fraction volume of brittle foreign particles and coarse eutectic domains, show the most strong stress oscillations of “plateau” stress level, as can be seen in Figure 2(b).

The high fraction volume of coarse brittle redundant phase, large brittle particles of partly converted TiH_2 , and particles/layers $\text{Al}_2\text{Ti}/\text{Al}_3\text{Ti}$ impair cell ductility and toughness. In addition, the presence of high fraction volume of foreign strong particles results in relatively high stresses required for hydride kinds of Al-Zn-Mg foams (F11, F12) to commence densification. Because of this undesirable high peak stress at the onset of global collapse followed by strong load drop causes the plateau stress for the above kinds of Al-foams to saddle shape. The presence of foreign Ca-bearing zones within the domains in the cell wall material of Al-foam (F11) causes the compression strength to decrease, although the shape of stress-strain curve remains rather similar to that for hydride kind of Al-foam (F12) fabricated without Ca. The application of CaCO_3 foaming agent provides a remarkable improvement of deformation pattern Al-foam (F14) based on Al-Zn-Mg alloy. Figure 2(b) demonstrates that carbonate Al-foam based on Al-Zn-Mg alloy processed without Ca shows much smoother stress-curve which keeps peak-to-peak amplitude of oscillations to minimum level.

Thus, a comparative analysis of compressive response for different kinds of Al-foams elucidate the fact that microstructure and mechanical damage of cell wall constituents have a dramatic effect on the microscopic mechanism of local

deformation and failure, which in turn is thought to have an influence on the macroscopic mechanical response of Al-foams. Brittle cell wall constituents such as brittle particles of partly converted TiH_2 rounded by an $\text{Al}_2\text{Ti}/\text{Al}_3\text{Ti}$ layer and smaller Al_3Ti particles as well as brittle eutectic domains/redundant phase act as likely sites for the initiation of cracks, propagation of which generates stress concentration in adjacent areas, intervening the Al-matrix, as can be seen in Figure 3. The final failure of cell walls apparently occurs by crushing the brittle cell constituents and their bridging across intact ligaments. Again, the local fracture of deformation bands causes oscillations of “plateau” stress, as shown in Figure 2.

3.3. Comparison of Al-Foam Compressive Strength with Theoretical Models. A comparison of experimental results outlined in this effort with theoretical predictions was fulfilled to estimate the role of cell wall microstructure and mechanical damage of cell wall constituents in mechanical performance of closed-cell Al-foams. Among several models based on idealized representation of a defect-free cellular structure the most famous relations applied for describing mechanical properties are published in [11, 19]. For open-cell foams made of elastic-plastic materials, dimensional arguments give the correlation of plastic collapse stress, σ_{pl} , relative to the yield strength of solid cell edge material, σ_{ys} , versus relative density, ρ/ρ_s , as [19]

$$\frac{\sigma_{\text{pl}}}{\sigma_{\text{ys}}} = C_3 \left(\frac{\rho}{\rho_s} \right)^n, \quad (1)$$

where $n = 3/2$ is power index and the constant C_3 related to cell geometry is roughly about 3 for a wide range of foams.

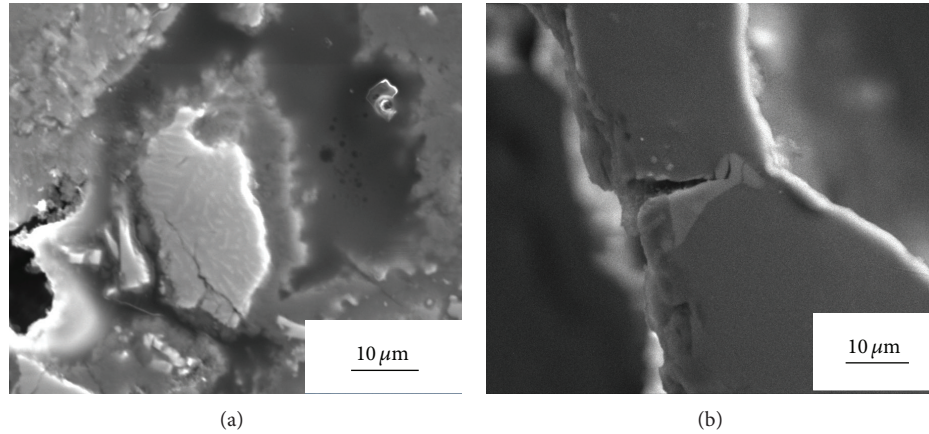


FIGURE 3: SEM images of the cell wall material for (a) hydride and (b) carbonate kinds of Al foams (F12, F13) based on Al-Zn-Mg alloy and performed (b) with (F13) and (a) without (F12) Ca additive: (a) cracks within partly converted TiH_2 , (b) crack lengthways the domain of redundant phase.

For closed-cell foams, yielding of stretched cell faces contribute to their strength. Because of this the additional term on right hand side appears in the relation for the plastic collapse stress:

$$\frac{\sigma_{\text{pl}}}{\sigma_{\text{ys}}} = C_3 \left(\frac{\rho}{\rho_s} \right)^n + C'_3 \left(\frac{\rho}{\rho_s} \right), \quad (2)$$

where power index $n = 1.5$.

For tetrakaidecahedral unit with flat faces, finite element analysis gives slightly different values in (2). According to [28] power index at the first term on the right hand side was found as $n = 2$ while the values of constants were determined as great as $C_3 = 0.33$ and $C'_3 = 0.44$.

Generally, compressive strength is usually defined either by “plateau” stress relative to the yield strength or by compressive strength at 20% strain [11]. Both yield stresses, σ_y , at the general yielding and plateau stress up to densification, σ_{pl} , [14] are used in the present study. Approximate values of yield strength, σ_{ys} , for solids which compositionally corresponded to the cell wall materials were determined by conventional mechanical tensile tests. The values of parameters σ_{ys} are listed in Table 1.

Following [11] data for the relative compression strength, $\sigma_y/\sigma_{\text{ys}}$ and $\sigma_{\text{pl}}/\sigma_{\text{ys}}$, for different kinds of Al-foams are plotted in Figure 4 along the lines representing (1) and (2). Figure 4(a) shows that the data for carbonate kind of Al-foam F2 processed with pure Al lie close to (2), as prescribed by the theory for closed-cell foams. However, a behavior of all the other kinds of Al-foams deviates more or less from theoretical predictions. Data for hydride kind of Al-foam (F1) processed with pure aluminum lie below (2) and shift to (1), as can be seen in Figure 4(a). Deviation of experimental results from theoretical predictions suggests the decreased contribution of plastic bending to failure.

The same is true for carbonate kind of Al-foam (F6) based on Al-7Si alloy and processed without Ca as well as for hydride kinds of Al-foams processed with alloys such as Al-7Si, Al-1Mg-0.6Si, and Al-5Mg and performed either

with (F8) or without (F10) Ca additive. Figure 4(b) shows that the data for yield stress of those Al-foams lie well below (2) and shifted to (1), whereas those for plateau stress lie close to the line representing strength for closed-cell foam. The discrepancy between (2) and the data for hydride kinds of Al-7Si foams (F3, F4) and carbonate kind of Al-7Si foam (F5) with Ca additive is the most pronounced. Figure 4(b) shows that the data for plateau stress of those Al-foams shift essentially below (2) while the data for yield stress lie either well below or at least along the line representing open-cell foam. Compressive behavior of hydride kinds of Al-foams (F7, F9), which were processed with alloys such as Al-1Mg-0.6Si and Al-5Mg and admixture of Ca, is very similar to that of Al-foams (F3, F5) based on Al-7Si alloy, which were processed either with TiH_2 or CaCO_3 and performed with Ca additive. The noticeable difference is only that the increased thickness of cell walls causes the compressive strength of Al-foams F7, F9 to shift upwards when relative density increases up to $\rho/\rho_s > 0.20$. Figure 4(a) shows that both kinds of Al-foams (F11–F14) processed with Al-Zn-Mg alloy exhibit the most deflection of the experimental results from theoretical predictions. The data for yield and plateau stresses of Al-foams (F11, F13, F14) shift well below the line representing open-cell foam, whereas those of Al-foam F12 lie close to (1).

Generally, one or another relation between compressive strength and relative density, ρ/ρ_s , could be adjusted to approximate compressive strength of each kind of Al-foams the same as it was shown recently [16]. For instance, the compressive strength of Al-foams (F1, F2) processed with pure Al complies reasonably well with relations prescribed by (2) for closed-cell structure. However, it is noticeable that the value of numerical coefficient C'_3 for Al-foam F1 is somewhat reduced as compared to that for Al-foam F2. This is usually associated with a contribution of fracture mode in the collapse of deformation bands. The same is true for carbonate kinds of Al-foams (F8, F10) processed alloys such as Al-1Mg-0.6Si and Al-5Mg. For other kinds of Al-foams (F3–F7, and F9) processed with alloys such as Al-7Si, Al-1Mg-0.6Si, and Al-5Mg the values of numerical coefficient C'_3

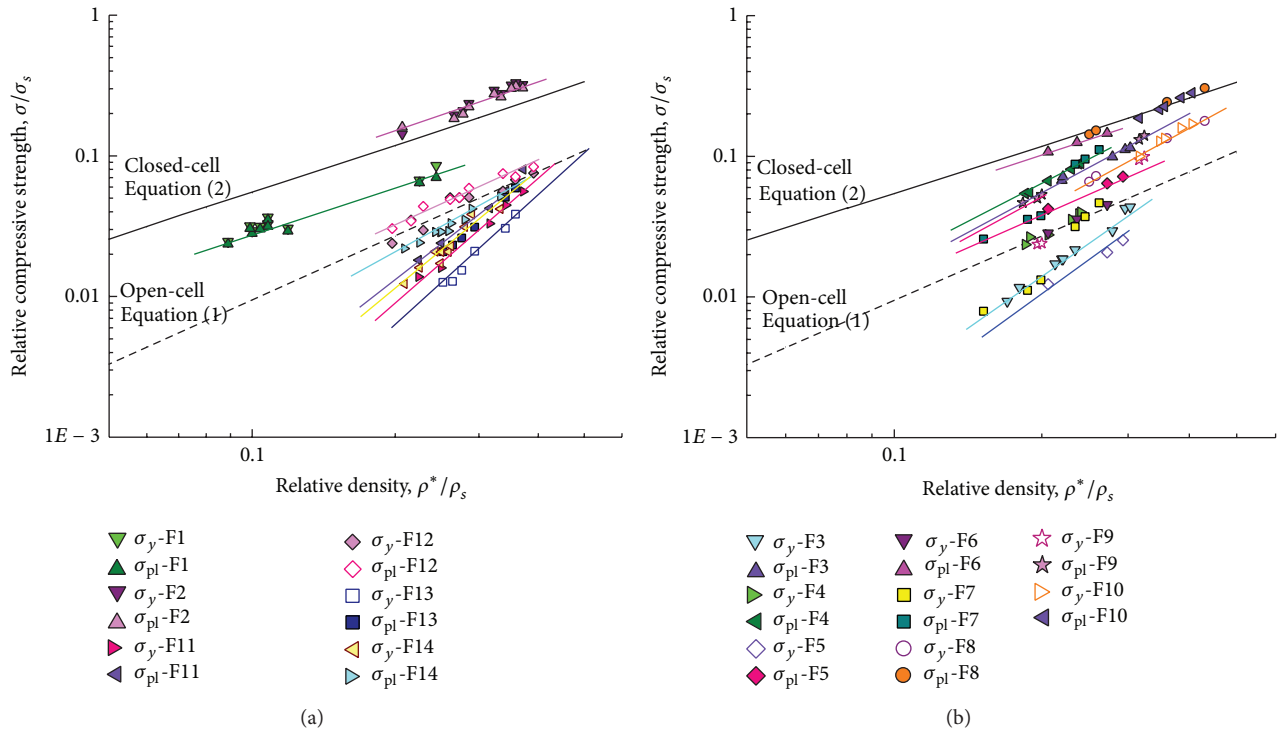


FIGURE 4: Relative compressive strength, σ_y/σ_{ys} and σ_{pl}/σ_{ys} , plotted against relative density, ρ/ρ_s , for different kinds of hydride (F1, F3, F4, and F7–F12) and carbonate (F2, F5, F6, F13, and F14) kinds of Al/Al alloy foams performed with (F1–F3, F5, F7, F9, F11, and F13) and without (F4, F6, F8, F10, F12, and F14) Ca additive: (a) Al-foams processed with Al (F1 and F2) and Al-foams of Al-Zn-Mg alloy (F11–F14); (b) Al-foams of Al alloys such as Al-7Si (F3–F6), Al-1Mg-0.6Si (F7 and F8), and Al-5Mg (F9 and F10).

relating to plateau stress are drastically reduced as compared to that prescribed by (2). Moreover, the numerical coefficient C_3' relating to yield stress for the above foams is completely degraded up to zero. The results of approximation show that strength degradation for Al-foams (F11–F14) processed with Al-Zn-Mg alloy is rather strong. Besides the values of numerical coefficient C_3' relating to yield and plateau stresses degraded up to zero, power index at the first term of (2) rises up to $n = 3$.

Thus, discrepancies of actual compressive strength for Al-foams and theoretical predictions reflect the difference in their micromechanism of deformation. By considering the evidence above it is easy to show that damage behavior of the cell wall constituents affects primary micromechanism of deformation, favoring either plastic buckling or brittle failure of the cell walls. Compressive stress, whose Al-foams can undergo up to densification, is proved to be actually very sensitive to small defects induced by crushed brittle constituents in the cell wall microstructure. An attention should be paid to the fact that effect of brittle constituents in the cell wall material on degradation of strength properties is much stronger. As it can be seen in Figure 4, the latter is comparable with that implemented by decreasing a relative density of intact Al-foam that is free of defects.

4. Conclusions

Crucial role of foaming agent and Ca additive in contaminations of the cell wall material by side products and, hence,

in macroscopic mechanical response of closed-cell Al-foams being fabricated via Alporas like route was justified.

Correlations of relative compressive strength, σ/σ_{ys} , versus relative density ρ/ρ_s , were obtained and analyzed. No discrepancy between experimental values of compressive strengths for Al-foams comprising ductile cell wall constituents and those prescribed by theoretical models based on an idealized representation of defect-free cellular structure for closed-cell structure is found while the opposite was believed to be true in the presence of low ductile and/or brittle processing contaminations including particles/layers of Al_3Ti , residues of partially reacted TiH_2 , Ca-bearing compounds, and/or modified eutectic domains. The latter contaminations result in reducing the compressive strength to values close to or even below those of open-cell foams of the same relative density, ρ/ρ_s . Considerable discrepancy of actual compressive strength of Al-foams and theoretical predictions resulted from difference in micromechanism of deformation, which, in turn, is affected by damage behavior of the cell wall constituents, favoring either plastic buckling or brittle failure of the cell walls.

The results of this work bring about a better understanding of the interplay between processing conditions, cell wall microstructure, damage behavior of cell wall constituents, and mechanical response of Al-foams.

Conflict of Interests

The authors declare that there is no conflict of interests regarding the publication of this paper.

Acknowledgments

This research was supported by National Academy of Science of Ukraine under the Project no. III-2-13. Special thanks are due to the researchers of Tohoku University, Japan, for fruitful discussions and cooperation.

References

- [1] M. F. Ashby, A. G. Evans, N. A. Fleck, L. J. Gibson, J. W. Hutchinson, and H. N. G. Wadley, *Metal Foams: A Design Guide*, Butterworth Heinemann, Boston, Mass, USA, 2000.
- [2] A. E. Markaki and T. W. Clyne, "Characterisation of impact response of metallic foam/ceramic laminates," *Materials Science and Technology*, vol. 16, no. 7-8, pp. 785–791, 2000.
- [3] V. Crupi, G. Epasto, and E. Guglielmino, "Impact response of aluminum sandwiches for light-weight ship structures," *Metals*, vol. 1, pp. 98–112, 2011.
- [4] J. Banhart, "Manufacture, characterisation and application of cellular metals and metal foams," *Progress in Materials Science*, vol. 46, no. 6, pp. 559–632, 2001.
- [5] R. Neugebauer, J. Hipke, T. Hohlfeld, and R. Thummler, "Highly damped machine tools with metal foam," in *Proceedings of the International Conference Advanced Metallic Materials*, J. Jerz, Ed., pp. 214–218, Institute of Materials and Machine Mechanics, Smolenice, Slovakia, November 2003.
- [6] T. Nakamura, S. V. Gnyloskurenko, K. Sakamoto, A. V. Byakova, and R. Ishikawa, "Development of new foaming agent for metal foam," *Materials Transactions*, vol. 43, no. 5, pp. 1191–1196, 2002.
- [7] V. Gergely, D. C. Curran, and T. W. Clyne, "The FOAMCARP process: foaming of aluminium MMCs by the chalk-aluminium reaction in precursors," *Composites Science and Technology*, vol. 63, no. 16, pp. 2301–2310, 2003.
- [8] S. Gnyloskurenko, T. Tnakamura, A. Byakova, Y. Podrezov, R. Ishikawa, and M. Maeda, "Development of lightweight al alloy and technique," *Canadian Metallurgical Quarterly*, vol. 44, no. 1, pp. 7–12, 2005.
- [9] A. Byakova, A. Sirko, K. Mykhalekov, Y. Milman, S. Gnyloskurenko, and T. Nakamura, "Improvements in stabilisation and cellular structure of Al based foams with novel carbonate foaming agent," *High Temperature Materials and Processes*, vol. 26, no. 4, pp. 239–245, 2007.
- [10] J. Banhart, "Light-metal foams history of innovation and technological challenges," *Advanced Engineering Materials*, vol. 15, no. 3, pp. 82–111, 2013.
- [11] L. J. Gibson, "Mechanical behavior of metallic foams," *Annual Review of Materials Science*, vol. 30, pp. 191–227, 2000.
- [12] A. E. Markaki and T. W. Clyne, "The effect of cell wall microstructure on the deformation and fracture of aluminium-based foams," *Acta Materialia*, vol. 49, no. 9, pp. 1677–1686, 2001.
- [13] T. Miyoshi, T. Mukai, and K. Higashi, "Energy absorption in closed-cell Al-Zn-Mg-Ca-Ti foam," *Materials Transactions*, vol. 43, no. 7, pp. 1778–1781, 2002.
- [14] A. V. Byakova, S. V. Gnyloskurenko, A. I. Sirko, Y. V. Milman, and T. Nakamura, "The role of foaming agent in structure and mechanical performance of Al based foams," *Materials Transactions*, vol. 47, no. 9, pp. 2131–2136, 2006.
- [15] Y. Milman, A. Byakova, A. Sirko, S. Gnyloskurenko, and T. Nakamura, "Improvement of structure and deformation behaviour of high strength Al-Zn-Mg foam," *Materials Science Forum*, vol. 519–521, no. 1, pp. 573–578, 2006.
- [16] A. Byakova, S. Gnyloskurenko, and T. Nakamura, "The role of foaming agent and processing route in the mechanical performance of fabricated aluminum foams," *Metals*, vol. 2, no. 2, pp. 95–112, 2012.
- [17] S. Akiyama, H. Ueno, K. Imagawa et al., "Foamed metal and method of producing same," US Patent no. 4713277, 1987.
- [18] A. V. Byakova, A. Vlasov, S. V. Gnyloskurenko, and I. Kartuzov, "Method for making the blocks of foamed aluminum/aluminum alloys," UA Patent no. 104367, 2014.
- [19] L. G. Gibson and M. F. Ashby, *Cellular Solids: Structure and Properties*, Cambridge University Press, Cambridge, UK, 1997.
- [20] W. E. Warren and A. M. Kraynik, "The linear elastic properties of open-cell foams," *Journal of Applied Mechanics*, vol. 55, no. 2, pp. 341–346, 1988.
- [21] H. X. Zhu, J. F. Knott, and N. J. Mills, "Analysis of the elastic properties of open-cell foams with tetrakaidecahedral cells," *Journal of the Mechanics and Physics of Solids*, vol. 45, no. 3, pp. 319–343, 1997.
- [22] W. E. Warren and A. M. Kraynik, "Linear elastic behavior of a low-density Kelvin foam with open cells," *Journal of Applied Mechanics*, vol. 64, no. 4, pp. 787–794, 1997.
- [23] N. J. Mills and H. X. Zhu, "The high strain compression of closed-cell polymer foams," *Journal of the Mechanics and Physics of Solids*, vol. 47, no. 3, pp. 669–695, 1999.
- [24] A. M. Kraynik, "The structure of random foam," in *Proceedings of the 4th International Conference on Porous Metals and Metal Foaming Technology (MetFoam '05)*, H. Nakajima and N. Kanetake, Eds., pp. 397–402, The Japan Institute of Metals, Kyoto, Japan, September 2005.
- [25] J. L. Grenestedt and F. Bassinet, "Influence of cell wall thickness variations on elastic stiffness of closed-cell cellular solids," *International Journal of Mechanical Sciences*, vol. 42, no. 7, pp. 1327–1338, 2000.
- [26] Y. Sugimura, J. Meyer, M. Y. He, H. Bart-Smith, J. Grenstedt, and A. G. Evans, "On the mechanical performance of closed cell al alloy foams," *Acta Materialia*, vol. 45, no. 12, pp. 5245–5259, 1997.
- [27] H. Bart-Smith, A.-F. Bastawros, D. R. Mumm, A. G. Evans, D. J. Speck, and H. N. G. Wadley, "Compressive deformation and yielding mechanisms in cellular Al alloys determined using X-ray tomography and surface strain mapping," *Acta Materialia*, vol. 46, no. 10, pp. 3583–3592, 1998.
- [28] A. E. Simone and L. J. Gibson, "The effects of cell face curvature and corrugations on the stiffness and strength of metallic foams," *Acta Materialia*, vol. 46, no. 11, pp. 3929–3935, 1998.
- [29] H. Harders, K. Hupfer, and J. Rösler, "Influence of cell wall shape and density on the mechanical behaviour of 2D foam structures," *Acta Materialia*, vol. 53, no. 5, pp. 1335–1345, 2005.
- [30] I. Jeon and T. Asahina, "The effect of structural defects on the compressive behavior of closed-cell Al foam," *Acta Materialia*, vol. 53, no. 12, pp. 3415–3423, 2005.
- [31] A. Marmottant, J. F. Despois, L. Salvo, E. Maire, M. Bornert, and A. Mortensen, "In-situ X-ray tomography investigation of replicated aluminium foam: quantitative analysis of localization using 3D strain mapping," in *Proceedings of the 4th International Conference on Porous Metals and Metal Foaming Technology (MetFoam '05)*, H. Nakajima and N. Kanetake, Eds., pp. 415–418, The Japan Institute of Metals, Kyoto, Japan, September 2005.
- [32] Y. Yamada, T. Banno, Z. Xie, and C. Wen, "Characterisation of aluminium foams using X-ray tomography," in *Proceedings of the 4th International Conference on Porous Metals and Metal Foaming Technology (MetFoam '05)*, H. Nakajima and

- N. Kanetake, Eds., pp. 419–422, The Japan Institute of Metals, Kyoto, Japan, September 2005.
- [33] H. Toda, N. Kuroda, and T. Ohgaki, “Image-based mechanical analysis of dynamic deformation and damage behaviors in an aluminum foam using synchrotron X-ray microtomography,” in *Proceedings of the 4th International Conference on Porous Metals and Metal Foaming Technology (MetFoam '05)*, H. Nakajima and N. Kanetake, Eds., pp. 409–414, The Japan Institute of Metals, Kyoto, Japan, September 2005.
- [34] B. Kriszt, B. Foroughi, K. Faure, and H. P. Degischer, “Behaviour of aluminium foam under uniaxial compression,” *Materials Science and Technology*, vol. 16, no. 7-8, pp. 792–796, 2000.
- [35] C. Chen, T. J. Lu, and N. A. Fleck, “Effect of imperfections on the yielding of two-dimensional foams,” *Journal of the Mechanics and Physics of Solids*, vol. 47, no. 11, pp. 2235–2272, 1999.
- [36] S. V. Gnyloskurenko, A. V. Byakova, A. I. Sirko, A. O. Dudnyk, and V. Yu. Milman, “Advanced structure and deformation pattern of Al based foamed with calcium carbonate agent,” in *Proceedings of the 5th International Conference on Porous Metals and Metallic Foams (MetFoam '07)*, L. P. Lefebvre, J. Banhart, and D. C. Dunand, Eds., pp. 399–402, DEStech Publication, Montreal, Canada, September 2007.



Hindawi

Submit your manuscripts at
<http://www.hindawi.com>

